INSTITUTE OF PHYSICS PUBLISHING PHYSICS IN MEDICINE AND BIOLOGY

Phys. Med. Biol. **49** (2004) 3979–3989 PII: S0031-9155(04)80369-5

Photon migration in turbid media with anisotropic optical properties

Olga K Dudko[1], **George H Weiss**[1], **Victor Chernomordik**[2] **and Amir H Gandjbakhche**[2]

[1] Mathematical and Statistical Computing Laboratory, Center for Information Technology, National Institutes of Health, Bethesda, MD 20892, USA
[2] Laboratory of Integrative and Medical Biophysics, National Institute of Child Health and Human Development, National Institutes of Health, Bethesda, MD 20892, USA

Received 4 May 2004
Published 6 August 2004
Online at stacks.iop.org/PMB/49/3979
doi:10.1088/0031-9155/49/17/011

Abstract

We analyse properties of photon migration in reflectance measurements made on a semi-infinite medium bounded by a plane, in which optical parameters may vary in directions neither parallel to, nor perpendicular to the bounding plane. Our aim in doing this is to develop the formulae necessary to deduce parameters of directionality from both time-gated and continuous wave measurements. The mathematical development is based on a diffusion picture, in which the bounding plane is regarded as being totally absorbing so that all photons reaching the surface contribute to the reflectance.

1. Introduction

A recent paper has analysed several effects of anisotropic optical properties on the migration of photons in a turbid medium (Dagdug *et al* 2003). Our analysis is motivated by biomedical applications to optical tissue properties, e.g., muscle, skin, white matter in the brain and dentin. Such tissues are characterized by anisotropic optical properties since scattered photons propagate preferentially along the fibres. The appropriate imaging and spectroscopic techniques were discussed recently in Nickell *et al* (2000) and Kienle *et al* (2003). The migration of photons in Dagdug *et al* (2003) was modelled in terms of a nearest-neighbour continuous time random walk (CTRW) (Weiss 1994). In that analysis the interior of the medium is represented by a simple cubic lattice bounded by one or two parallel planes able to absorb photons and convert them to observable light. Measurements of light re-emitted from the absorbing plane or planes provide data needed to estimate optical parameters of the tissue interior. The earlier theory in Dagdug *et al* (2003) has been successfully applied to experiments carried out by Sviridov *et al* (2004) in which intensity profiles of linearly polarized light backscattered from skin and tissue-like phantoms were measured. These investigators

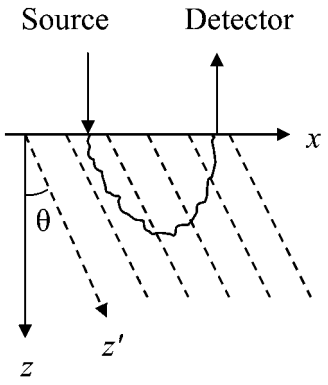

Figure 1. Schematic diagram of both the time-gated and cw measurements, for simplicity drawn in two dimensions. The optical parameters lie along the dashed lines which are canted at an angle θ from the z-axis.

showed that, by analysing polarization measurements, in all cases considered, i.e., a delrin slab, demineralized bone, mice and human skin, almost all of the backscattered photons detected at distances of greater than 1 to 2 mm from the entry point had experienced multiple scattering events, thus validating the use of diffusion or random walk models. Comparison of the experimental data with formulae for backscattered intensity distributions given in Dagdug *et al* (2003) allowed the investigators to estimate the scattering coefficients parallel and perpendicular to the fibres.

In models based on diffusion or random walk theory, the absorbing boundary in the case of a semi-infinite medium is the plane defined by $z = 0$. By convention, positive z corresponds to points in the interior of the tissue. A transport-theory-based analysis concentrating on parameters other than those considered in this note is to be found in a paper by Heino *et al* (2002). The model described in Dagdug *et al* (2003) assumes that the laser radiation impinges on the planar boundary along an axis perpendicular to the plane boundary. However, optical properties of tissue cannot always be assumed to be these special configurations. Consequently, a more general model would seem to be useful in the application of optical methods in biomedical applications.

The formalism based on the CTRW has the advantage that, with a proper choice of pausing-time density and the random walk defined on a simple cubic lattice, the model can be solved exactly (Weiss *et al* 1998). This greatly simplifies the exploration of optical parameters required to interpret experimental results. However, the most useful set of results, from the qualitative point of view, is obtained by passing to the diffusion limit as in Dagdug *et al* (2003), in which case the mathematical description of the anisotropy is based on the use of a diagonal diffusion tensor whose nonzero elements are allowed to differ from one another. In this paper we show how the theory described in Dagdug *et al* (2003) can be generalized to apply to cases in which the optical properties are constant in directions differing from those parallel to the coordinate axes. As in Dagdug *et al* (2003), in order to simplify the analysis, we consider only the special case in which two of the three elements of the diffusion tensor are equal. A straightforward extension of the results given here can be developed to treat the more general case in which all three of the tensor elements are allowed to differ.

In time-gated experiments, at a fixed position of the detector, a laser pulse enters the tissue and the reflectance response is measured as a function of time. In the continuous wave (cw) experiment a continuous laser beam is used and measurements of reflectance are made as a function of distance. In figure 1 the anisotropy is illustrated by the dashed lines, and

the angle θ is measured with respect to the z-axis. In three dimensions there can be at least two more angles so that in the most general case there are three different probabilities. We will not analyse this most general model that takes three angles into account, but assume, as a simplification, that two of the angles are equal.

The rest of the paper is divided into two major sections. Section 2 contains a derivation of the propagator that characterizes photon trajectories in the system which is the basis for predicting the pattern of photon reflectance both in time-gated experiments and in cw measurements. In section 3 we use the expression for the propagator to suggest techniques for estimating underlying properties of the optical parameters.

2. Derivation of reflectance in time-gated measurements

2.1. Definition of parameters

To define the physical system, the position of a point in the laboratory frame of reference will be denoted by $\mathbf{r} = (x, y, z)$. The plane defined by $z = 0$ is an interface between the tissue and the exterior, with values of $z > 0$ pointing into the medium, while x and y are the coordinates transverse to the z-axis. The two optical parameters describing optical properties of the assumed homogeneous tissue are μ_s', the transport-corrected scattering coefficient, and μ_a, the absorption coefficient. The validity of the Beer–Lambert law will be assumed. This means that the probability of migrating within the tissue for a dimensionless time τ without being absorbed internally is $\exp(-\nu\tau)$, where $\tau = kt$ is a dimensionless time, the parameter k being the inverse of the mean time between successive scatterings. The dimensionless absorption parameter, ν, is related to the two optical coefficients by $\nu = \mu_a/\mu_s'$.

We wish to describe and analyse a system whose optical properties are rotated with respect to the absorbing interface. To do so, one starts by defining a point in space in terms of a coordinate system determined by the directions of the optical parameters. A point in this skewed coordinate system is defined by an affine transformation of the laboratory frame of reference. A point in the rotated coordinate system will be denoted by $\mathbf{r}' = (x', y', z')$.

2.2. The diffusion tensor

In this section we provide the theoretical infrastructure allowing us to express properties of the optical parameters in terms of measurements of $I(\mathbf{R}, \tau)$, the reflectance through the tissue surface that appears at a target point $\mathbf{R} = (X, Y, 0)$, at time τ. Let the two equal diffusion constants in the skewed coordinates be denoted by $D_{x'}(= D_{y'})$ and let the third be $D_{z'} = BD_{x'}$, where the parameter B will be termed the bias parameter. This is a measure of the diffusive spreading along the z'-axis as opposed to that along the remaining two axes. The diffusion constant $D_{x'}$, as is standard, is related to the scattering coefficient as $D_{x'} = (3\mu_s')^{-1}$. The diffusion tensor is therefore of the form

$$\mathbf{D}' = \begin{pmatrix} D_{x'} & 0 & 0 \\ 0 & D_{x'} & 0 \\ 0 & 0 & D_{z'} \end{pmatrix} = D_{x'} \begin{pmatrix} 1 & 0 & 0 \\ 0 & 1 & 0 \\ 0 & 0 & B \end{pmatrix} \tag{2.1}$$

so that $B = 1$ corresponds to isotropic diffusion. When $B > 1$ diffusive propagation tends to be more pronounced along the z'-axis than along the x' and y' axes while $B < 1$ implies slower propagation along the z'-axis.

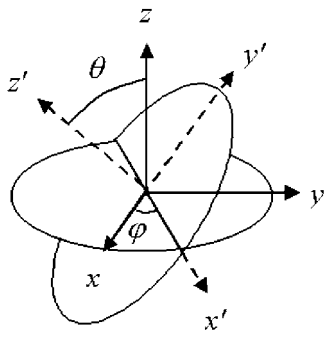

Figure 2. Schematic diagram defining the rotation angles φ and θ.

2.3. Relating laboratory and rotated coordinates

A first step in deriving an expression for the propagator is to derive a transformation matrix, **M**, taking one from the laboratory frame of reference to the rotated set of coordinates. In figure 2 we define the rotation angles φ and θ as respectively being a rotation around the z-axis followed by one around either the x or y axis. This matrix is to be inserted into the relation $\mathbf{r}' = \mathbf{M}\mathbf{r}$, where $\mathbf{r}'$ is a position vector in the rotated coordinate system, and $\mathbf{r}$ is the corresponding one in the laboratory system. The precise form of the transformation is found by multiplying two rotation matrices together (Goldstein 1950):

$$\mathbf{M} = \mathbf{M}_\theta \mathbf{M}_\varphi \tag{2.2}$$

where

$$\mathbf{M}_\theta = \begin{pmatrix} 1 & 0 & 0 \\ 0 & c_\theta & s_\theta \\ 0 & -s_\theta & c_\theta \end{pmatrix} \qquad \mathbf{M}_\varphi = \begin{pmatrix} c_\varphi & s_\varphi & 0 \\ -s_\varphi & c_\varphi & 0 \\ 0 & 0 & 1 \end{pmatrix}. \tag{2.3}$$

To make the notation more compact we have abbreviated the trigonometric functions by writing $c_\theta = \cos\theta, s_\theta = \sin\theta$, and so forth. Equation (2.2) is explicitly written as the composite transformation equations

$$\begin{aligned} x' &= xc_\varphi + ys_\varphi \\ y' &= -xc_\theta s_\varphi + yc_\theta c_\varphi + zs_\theta \\ z' &= xs_\theta s_\varphi - ys_\theta c_\varphi + zc_\theta \end{aligned} \tag{2.4}$$

with the corresponding inverse relations

$$\begin{aligned} x &= x'c_\varphi - y'c_\theta s_\varphi + z's_\theta s_\varphi \\ y &= x's_\varphi + y'c_\theta c_\varphi - z's_\theta c_\varphi \\ z &= y's_\theta + z'c_\theta. \end{aligned} \tag{2.5}$$

The new set of coordinate axes, rotated with respect to the laboratory frame of reference, establishes a one-to-one relation between points in the laboratory coordinates and those in the rotated frame of reference. It was shown in Dagdug *et al* (2003) that the asymptotic forms of both the propagators and the measured surface intensity as functions of the spatial parameters are spatially uncorrelated when expressed in terms of laboratory coordinates. It should be noted that the matrix **M** corresponds to a rotation first around the z-axis followed by a rotation around the y-axis. The most important coordinate system from the physical

point of view is the laboratory coordinate system, which is the only one accessible to the experimenter who initially has no information related to the directionality of the optical parameters. Measurements of surface reflectance intensity provide data from which, in theory, it is possible to estimate optical properties of the medium.

2.4. Solution for the propagator

A standard solution to the diffusion equation in the rotated coordinate system can be found assuming that the initial condition is $\mathbf{r}_0 = (0, 0, z_0)$ where the unit of length, z_0, can be taken to be a scattering length. By appealing to equation (2.4) we see that the corresponding quantity in the rotated coordinates is

$$\mathbf{r}'_0 = (0, z_0 s_\theta, z_0 c_\theta). \tag{2.6}$$

An exact solution for the free-space propagator in the rotated coordinate system is

$$p^{(F)}(\mathbf{r}', \tau|\mathbf{r}'_0) = \left(\frac{1}{4\pi D_{x'}\tau}\right)^{3/2} \frac{1}{B^{1/2}} \exp\left\{-\frac{1}{4D_{x'}\tau}[(x')^2 + (y' - z_0 s_\theta)^2 + (z' - z_0 c_\theta)^2/B] - \nu\tau\right\} \tag{2.7}$$

which is essentially the propagator for the standard diffusion equation provided that B is incorporated into the term in brackets, as is done in the preceding equation. An expression for the exponent in equation (2.7) in terms of laboratory coordinates is given in appendix A.

To take the absorbing boundary into account we require that the probability density for the displacement at time τ, expressed in terms of laboratory coordinates, should vanish when $z = 0$. It follows from equation (2.5) that in the rotated coordinates the plane on which we require the probability density to vanish is the solution to $y' s_\theta + z' c_\theta = 0$ or

$$z' = -y' t_\theta \tag{2.8}$$

where $t_\theta = \tan\theta$. To convert the free-space propagator to one satisfying the boundary condition at $z = 0$ one needs to subtract from equation (2.7) a solution to the diffusion equation to ensure that the difference vanishes when equation (2.8) is satisfied. Let this second solution be denoted by $q(\mathbf{r}'; \tau)$ which we write as

$$q(\mathbf{r}'; \tau) = \frac{1}{(4\pi D_{x'}\tau)^{3/2}} \exp\left\{-\frac{(x')^2 + (y' - z_0 U)^2 + (y' t_\theta + z_0 V)^2/B}{4D_{x'}\tau} - \nu\tau\right\} \tag{2.9}$$

where U and V are constants which are determined by requiring that the propagator vanish on the surface

$$p^{(F)}(\mathbf{r}'; \tau) - q(\mathbf{r}'; \tau) = 0 \tag{2.10}$$

when equation (2.8) is satisfied.

Our ultimate goal is to express the propagator and surface intensity in laboratory coordinates since the only information available from experiments is found from the reflectance. In performing the derivation it will prove convenient to introduce a parameter Ω by

$$\Omega = 1 - \frac{1}{B} \tag{2.11}$$

so that $B = 1$, the isotropic case, corresponds to $\Omega = 0$. After some algebra, one finds that the parameters U and V in equation (2.9) are

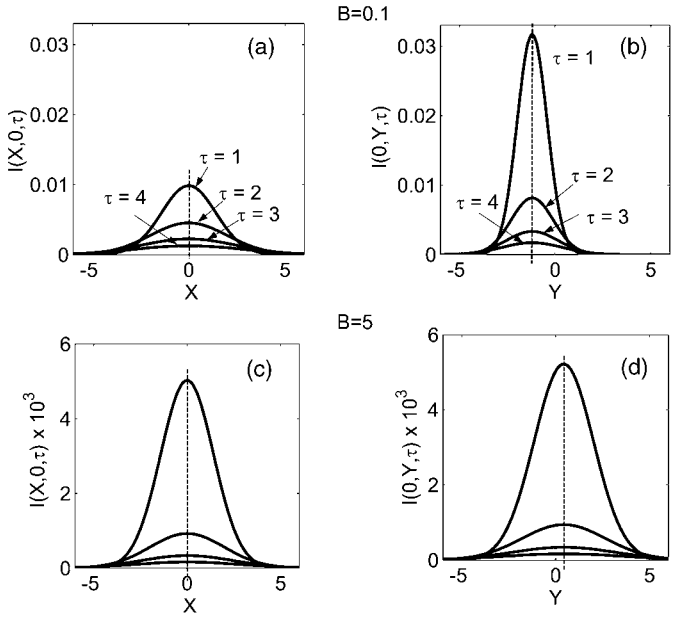

Figure 3. Evolution of the intensities as a function of time in a time-gated experiment for two values of the bias, $B = 0.1$ and $B = 5$. The parameter values used in generating the curves are $z_0 = 1, \varphi = 0, \theta = \pi/6$ rad.

$$U = \frac{s_\theta\left[\Omega\left(1 + c_\theta^2\right) - 1\right]}{1 - \Omega s_\theta^2} \qquad V = -\frac{c_\theta\left[1 + \Omega s_\theta^2\right]}{1 - \Omega s_\theta^2}. \tag{2.12}$$

The denominator in these expressions cannot vanish since $1 - \Omega s_\theta^2 = c_\theta^2 + s_\theta^2/B$ is always positive.

2.5. The surface intensity

Any estimate of the underlying parameters must be based on the reflectance at the surface. The surface intensity at point $\mathbf{R} = (X, Y, 0)$ at time τ will be identified as the flux of photons through the interface. This intensity can be found from the relation

$$I(\mathbf{R}; \tau) = -D_x \left.\frac{\partial p}{\partial z}\right|_{z=0} \tag{2.13}$$

which can be expressed in terms of the rotated coordinates as

$$I(\mathbf{R}; \tau) = -D_x \left(s_\theta \left.\frac{\partial p}{\partial y'}\right|_{z'=-y't_\theta} + c_\theta \left.\frac{\partial p}{\partial z'}\right|_{z'=-y't_\theta} \right). \tag{2.14}$$

The expression for $I(\mathbf{R}; \tau)$ which follows from this equation is quite complicated. It is given as a function of the angles and bias in appendix B. However, the expression given there can be simplified by observing that the scattering length z_0 will generally be small in comparison with other lengths that describe the system. Figure 3 contains curves of the re-emitted intensity as a function of distance for different values of time. This is taken from equation (2.14) for a sampling of different parameters.

If we include the parameter z_0 explicitly in the expression for the intensity, writing it as $I(\mathbf{R}; \tau|z_0)$, we observe that this function must vanish when $z_0 = 0$. Hence we can expand

$I(\mathbf{R};\tau|z_0)$ around $z_0 = 0$ and retain only the first term which is proportional to z_0. The result of doing so produces

$$I(\mathbf{R};\tau|z_0) \approx z_0 \left.\frac{\partial I(\mathbf{R};\tau|z_0)}{\partial z_0}\right|_{z_0=0} = \frac{z_0 \exp\left[-\frac{1}{4D_{x'}\tau}\mathbf{RQR}' - \nu\tau\right]}{(4\pi D_{x'})^{3/2}\left(1 + B\Omega c_\theta^2\right)\tau^{5/2}} \tag{2.15}$$

in which $\mathbf{Q}$ is the 2×2 matrix

$$\mathbf{Q} = \begin{pmatrix} 1 - s_\varphi^2 s_\theta^2 \Omega & c_\varphi s_\varphi s_\theta^2 \Omega \\ c_\varphi s_\varphi s_\theta^2 \Omega & 1 - c_\varphi^2 s_\theta^2 \Omega \end{pmatrix} \tag{2.16}$$

and $\mathbf{R}'$ is the transpose of $\mathbf{R}$. An expression for the quadratic form $\mathbf{RQR}'$ in terms of laboratory coordinates is

$$\mathbf{RQR}' = X^2\left(1 - \Omega s_\theta^2 s_\varphi^2\right) + 2XY\Omega s_\theta^2 c_\varphi s_\varphi + Y^2\left(1 - \Omega s_\theta^2 c_\varphi^2\right). \tag{2.17}$$

Since Ω takes values only in the range $(-\infty, 1)$ the diagonal elements of $\mathbf{Q}$ are always positive and, in fact, $\mathbf{Q}$ is positive definite for all values of B. Therefore, the equi-intensity contours in the exponential in equation (2.15) correspond to an ellipse. Figure 4(a) shows the rotation of the ellipse as a function of φ for $B = 0.1$, $B = 5$, angle θ fixed at $\pi/6$ rad, and $\tau = 10$. The value $B = 1$ or $\Omega = 0$ gives rise to a circle so that all dependence on the angles disappears. Figure 4(b) is the analogous figure for changes in eccentricity of the ellipse as a function of θ when φ is set equal to 0. It should be noted that the centre of the ellipse remains at the origin. In fact, there is a slight displacement of the centre of the ellipse from the origin, but this is a second-order effect, i.e., it is proportional to z_0^2 and consequently would be extremely difficult to measure with any accuracy.

3. Estimation of optical parameters

3.1. Diagonalization of $\mathbf{Q}$

When x, y axes are fixed on the surface it is possible to diagonalize the matrix $\mathbf{Q}$ in equation (2.16) to determine the angle between axes of the ellipse and those of the laboratory coordinate system. The rotation of the ellipse also yields the ratio of lengths of the semi-axes of the ellipse since these are just the diagonal elements of the rotated matrix.

Let the angle between the semi-axis of the ellipse and the X-axis be denoted by ξ. To find this angle we define new spatial variables by $\bar{X}$ and $\bar{Y}$, writing

$$X = \bar{X}c_\xi + \bar{Y}s_\xi \qquad Y = -\bar{X}s_\xi + \bar{Y}c_\xi. \tag{3.1}$$

The new coordinates lie along the two axes of the ellipse. The angle by which the ellipse is rotated, ξ, is found by substituting this transformation into $\mathbf{RQR}'$ and choosing ξ so as to eliminate the cross term $\bar{X}\bar{Y}$. Doing so leads to the result $\tan 2\xi = -\tan 2\varphi$ or $\xi = -\varphi$, so that the observed angle of rotation can only provide information about the rotation angle φ, but not about the remaining two initially unknown parameters, B or θ.

The equation

$$\mathbf{RQR}' = C^2 = \text{constant} \tag{3.2}$$

defines an ellipse the lengths of whose two semi-axes are C and $C\left/\left(c_\theta^2 + s_\theta^2/B\right)^{1/2}\right.$. Thus, the ratio of the lengths of the two semi-axes of the ellipse, $L_{\bar{X}}$ and $L_{\bar{Y}}$, is

$$\frac{L_{\bar{Y}}}{L_{\bar{X}}} = \frac{1}{\sqrt{1 - \Omega s_\theta^2}} = \sqrt{\frac{B}{Bc_\theta^2 + s_\theta^2}} \tag{3.3}$$

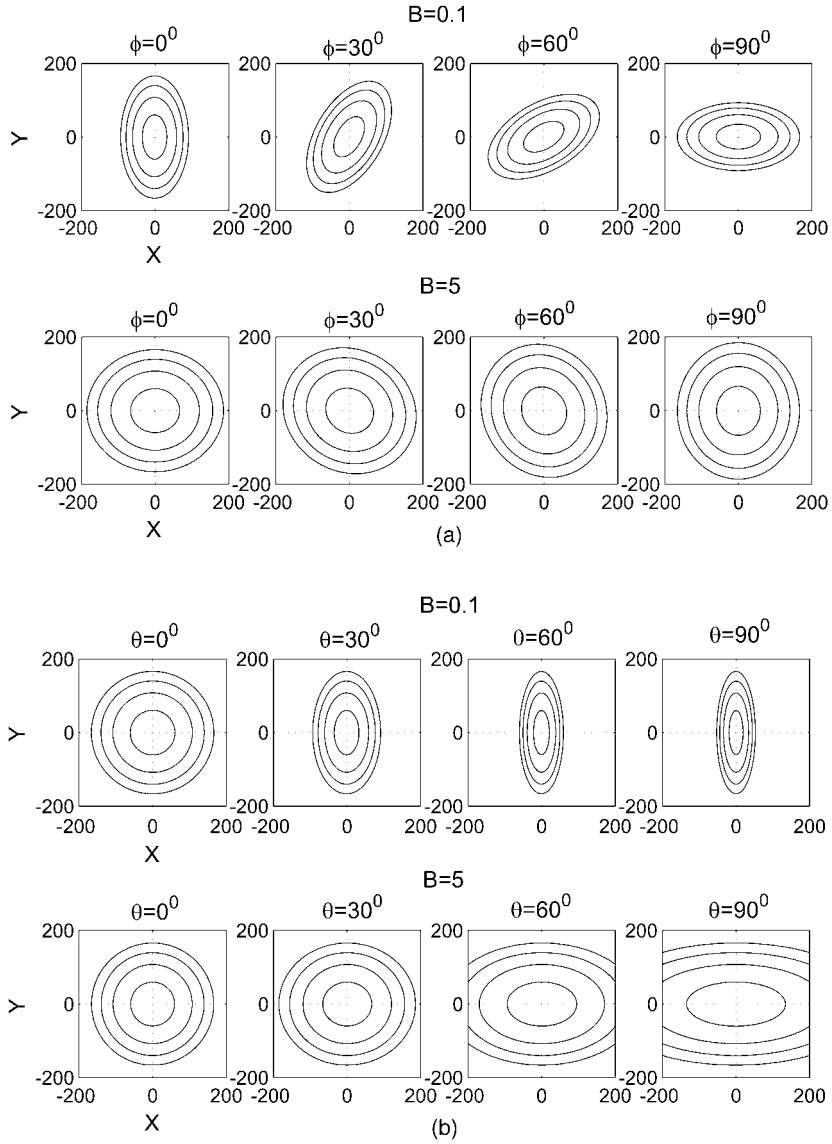

Figure 4. (a) Rotation of the ellipse of iso-intensity lines as a function of the angle φ when the angle θ is held fixed at 30° and for the values $B = 0.1$ and $B = 5$. (b) Rotation of the ellipse of iso-intensity lines as a function of θ when $\varphi = 0$. Here again $B = 0.1$ and $B = 5$.

or

$$1 - \Omega s_\theta^2 = (L_{\bar{X}}/L_{\bar{Y}})^2. \tag{3.4}$$

The relation in the last two equations depends on both B and θ and is independent of the parameter C in equation (3.2). Since the major and minor axes of the ellipse can be measured, we have an estimate of $1 - \Omega s_\theta^2$. A second equation containing these parameters must be found to provide an estimate of B and θ when $D_{x'}$ is known.

To provide this relation we observe that $I(\mathbf{R}; \tau|z_0)$ has a single maximum as a function of time τ, as may be confirmed from the relation in equation (2.15). Let this maximum occur

at $\tau_{\max}(\bar{X}, \bar{Y})$. If we expand the result in powers of ν, and retain only the constant term on the grounds that ν is generally quite small we find

$$\tau_{\max}(\bar{X}, \bar{Y}) \approx \frac{1}{10D_{x'}}\left[\bar{X}^2 + \bar{Y}^2\left(1 - \Omega s_\theta^2\right)\right] \tag{3.5}$$

which again depends only on the combination $1 - \Omega s_\theta^2$ so that $\tau_{\max}(\bar{X}, \bar{Y})$ has the same information related to B and θ as that provided by the ratio in equation (3.3). The parameter $D_{x'}$ can be estimated from this relation since the remaining terms depend only on the angle φ and $\left(1 - \Omega s_\theta^2\right)$. The surface intensity at the maximum is

$$\begin{aligned} I_{\max}(\mathbf{R};\, \tau|z_0) &\approx z_0 \frac{\exp\left(-\frac{\bar{X}^2 + \bar{Y}^2(1-\Omega s_\theta^2)}{4D_{x'}\tau_{\max}(\bar{X},\bar{Y})}\right)}{(4\pi D_{x'})^{3/2}\left(1 + B\Omega c_\theta^2\right)\tau_{\max}^{5/2}(\bar{X}, \bar{Y})} \\ &= z_0 \frac{\mathrm{e}^{-5/2}10^{5/2}D_{x'}}{(4\pi)^{3/2}B\left(1 - \Omega s_\theta^2\right)\left[\bar{X}^2 + \bar{Y}^2\left(1 - \Omega s_\theta^2\right)\right]}. \end{aligned} \tag{3.6}$$

Since the factor $1 - \Omega s_\theta^2$ is given in equation (3.4) where it is expressed in terms of the $(L_{\bar{X}}/L_{\bar{Y}})^2$ we may use this relation to find B in terms of the remaining parameters. Figure 3 shows some graphs of the surface intensity at two values of B. One sees from the four sets of curves that $I_{\max}(\mathbf{R};\, \tau|z_0)$ is approximately Gaussian and that there is a slight shift of the maxima of the curves, the direction of the shift depending on the bias. The value of B at which the crossover occurs is $B = 1$.

3.2. CW measurements

The reader will observe that all of the formulae given so far have been derived using the assumption that $D_{x'}$ is known. A second kind of measurement is required to determine this parameter. The measurements so far were time-gated. A simple alternative to this class of measurements is to make a continuous-wave experiment. That is to say, we return to equation (2.15) and integrate $I(\mathbf{R};\, \tau|z_0)$ with respect to τ. To express the result define the function

$$a = \frac{\mathbf{RQR}'}{D_{x'}}. \tag{3.7}$$

One then finds that

$$\int_0^\infty I(\mathbf{R};\, \tau|z_0)\,\mathrm{d}\tau = \frac{z_0}{(4\pi D_{x'})^{3/2}\left(1 + B\Omega c_\theta^2\right)}\frac{\sqrt{\pi\nu}}{a}\left[1 + \frac{1}{\sqrt{\pi a}}\right]\mathrm{e}^{-\sqrt{\nu a}}. \tag{3.8}$$

When νa is very small this reduces to

$$\int_0^\infty I(\mathbf{R};\, \tau|z_0)\,\mathrm{d}\tau \approx \frac{z_0}{4\pi D_{x'}\left(1 + B\Omega c_\theta^2\right)(\mathbf{RQR}')}. \tag{3.9}$$

The parameter $D_{x'}$ can be found from this equation as well as from equation (3.6). Although the preceding analysis has omitted the effects of internal absorption such effects are easily incorporated into the analysis at the cost of slightly more complicated formulae. The absorption is also relatively easy to estimate from the long-time behaviour of data from time-gated experiments.

4. Conclusions

We have shown that it is theoretically possible to estimate the two angles that define the anisotropy, as well as estimating the bias using a combination of time-gated and continuous-wave measurements. However, the changes in the surface intensity will sometimes depend only weakly on changes in angle as can be seen from figure 4. A more comprehensive study of the parameter space is therefore warranted. Finally, we note that the same techniques for analysing the consequences of anisotropy can be used to estimate optical parameters when the assumption that two of the transition probabilities are equal is dropped. The resulting theory essentially follows the analysis of the theory related to Eulerian angles as discussed in Goldstein (1950).

Appendix A. Terms of the exponential in equation (2.7)

The two components required for the evaluation of the exponential in equation (2.7) are

$$(x')^2 + (y' - z_0 s_\theta)^2 = x^2\left(c_\varphi^2 + c_\theta^2 s_\varphi^2\right) + y^2\left(s_\varphi^2 + c_\theta^2 c_\varphi^2\right) + (z - z_0)^2 s_\theta^2 + 2xy s_\theta^2 c_\varphi s_\varphi - 2x(z - z_0)c_\theta s_\theta s_\varphi + 2y(z - z_0)c_\theta s_\theta c_\varphi \tag{A1}$$

and

$$(z' - z_0 c_\theta)^2 = x^2 s_\theta^2 s_\varphi^2 + y^2 s_\theta^2 c_\varphi^2 + (z - z_0)^2 c_\theta^2 - 2xy s_\theta^2 c_\varphi s_\varphi + 2x(z - z_0)c_\theta s_\theta s_\varphi - 2y(z - z_0)c_\theta s_\theta c_\varphi. \tag{A2}$$

Appendix B. Exact expression for the surface intensity

The surface intensity is found in terms of the flux as given in equation (2.13) in which

$$\left.\frac{\partial p}{\partial z}\right|_{z=0} = \frac{1}{16\pi^{3/2}(4D_{x'}\tau)^{5/2}} \exp\left[-\frac{(xc_\varphi + yc_\varphi)^2}{4D_{x'}\tau} - \nu\tau\right]\{E_1(\theta, \varphi, \mathbf{R}) - E_2(\theta, \varphi, \mathbf{R})\} \tag{B1}$$

where the $E_i(\theta, \varphi)$ are

$$E_1(\theta, \varphi) = \left[\Omega c_\theta s_\theta (X s_\varphi - Y c_\varphi) + z_0\left(1 - \Omega c_\theta^2\right)\right] \times \exp\left\{-\frac{[(Xc_\theta s_\varphi - Yc_\theta c_\varphi + z_0 s_\theta)^2]}{4D_{x'}\tau} - \frac{\frac{1}{B}\{(Xs_\theta s_\varphi - Ys_\theta c_\varphi - z_0 c_\theta)^2\}}{4D_{x'}\tau}\right\} \tag{B2}$$

and

$$E_2(\theta, \varphi) = \left[\Omega c_\theta s_\theta (X s_\varphi - Y c_\varphi) + z_0\left(U s_\theta - \frac{V c_\theta}{B}\right)\right] \times \exp\left\{-\frac{[(Xc_\theta s_\varphi - Yc_\theta c_\varphi + z_0 U)^2]}{4D_{x'}\tau} - \frac{\frac{1}{B}\{(Xs_\theta s_\varphi - Ys_\theta c_\varphi + z_0 V)^2\}}{4D_{x'}\tau}\right\}. \tag{B3}$$

References

Dagdug L, Weiss G H and Gandjbakhche A H 2003 Effects of anisotropic optical properties on photon migration in structured tissues *Phys. Med. Biol.* **48** 1361–70

Gandjbakhche A H, Bonner R F and Nossal R 1992 Scaling relations for anisotropic random walks *J. Stat. Phys.* **69** 35–53

Gandjbakhche A H, Bonner R F and Nossal R 1993 Scaling relations for theories of anisotropic random walks applied to tissue optics *Appl. Opt.* **32** 504–16

Goldstein H 1950 *Classical Mechanics* (Cambridge, MA: Addison-Wesley)

Heino J, Arridge S, Sikora J and Somersalo E 2003 Anisotropic effects in highly scattering media *Phys. Rev.* E **68** 031098 8p

Heino J, Arridge S and Sommersalo E 2002 Anisotropic effect in light scattering and some implications in optical tomography *Tech. Dig. OSA Biomedical Topical Meetings* pp 18–20

Kienle A, Forster F K, Diebolder R and Hibst R 2003 Light propagation in dentin: influence of microstructure on anisotropy *Phys. Med. Biol.* **48** N7–14

Nickell S, Herman M, Ehrenpreis M, Farrell T J, Krämer U and Paterson M S 2000 Anisotropy of light propagation in human skin *Phys. Med. Biol.* **45** 2873–86

Sviridov A, Chernomordik V, Hassan M, Russo A, Eidsath A, Smith P and Gandjbakhche A H 2004 Intensity profiles of linearly polarized light backscattered from skin and tissue-like phantoms *J. Biomed. Opt.* at press

Weiss G H 1994 *Aspects and Applications of the Random Walk* (Amsterdam: Elsevier)

Weiss G H, Porrà J M and Masoliver J 1998 The continuous-time random walk description of photon motion in an isotropic medium *Opt. Commun.* **146** 268–76